

Spin-driven phonon splitting in bond-frustrated ZnCr₂S₄

Joachim Hemberger, T. Rudolf, Hans-Albrecht Krug von Nidda, Franz Mayr, Andrei Pimenov, Vladimir Tsurkan, Alois Loidl

Angaben zur Veröffentlichung / Publication details:

Hemberger, Joachim, T. Rudolf, Hans-Albrecht Krug von Nidda, Franz Mayr, Andrei Pimenov, Vladimir Tsurkan, and Alois Loidl. 2006. "Spin-driven phonon splitting in bond-frustrated ZnCr₂S₄." Physical Review Letters 97 (8): 087204. <https://doi.org/10.1103/physrevlett.97.087204>.

Nutzungsbedingungen / Terms of use:

licgercopyright

Dieses Dokument wird unter folgenden Bedingungen zur Verfügung gestellt: / This document is made available under the following conditions:

Deutsches Urheberrecht

Weitere Informationen finden Sie unter: / For more information see:

<https://www.uni-augsburg.de/de/organisation/bibliothek/publizieren-zitieren-archivieren/publizieren>



Spin-Driven Phonon Splitting in Bond-Frustrated ZnCr_2S_4

J. Hemberger,¹ T. Rudolf,¹ H.-A. Krug von Nidda,¹ F. Mayr,¹ A. Pimenov,¹ V. Tsurkan,^{1,2,*} and A. Loidl¹

¹*Experimental Physics V, Center for Electronic Correlations and Magnetism, University of Augsburg, D-86159 Augsburg, Germany*

²*Institute of Applied Physics, Academy of Sciences of Moldova, MD-2028 Chişinău, Republic of Moldova*

(Received 17 February 2006; published 22 August 2006)

Magnetic susceptibility, specific heat, thermal expansion, and IR spectroscopy provide experimental evidence that the two subsequent antiferromagnetic transitions in ZnCr_2S_4 at $T_{N1} = 15$ K and $T_{N2} = 8$ K are accompanied by significant thermal and phonon anomalies. The anomaly at T_{N2} reveals a temperature hysteresis typical for a first-order transformation. Because of strong spin-phonon coupling, both magnetic transitions at T_{N1} and T_{N2} induce a splitting of phonon modes. The anomalies and phonon splitting observed at T_{N2} are suppressed by strong magnetic field. Regarding the small positive Curie-Weiss temperature $\Theta \approx 8$ K, we argue that this scenario of two different magnetic phases with different magnetoelastic couplings results from the strong competition of ferromagnetic and antiferromagnetic exchange.

DOI: [10.1103/PhysRevLett.97.087204](https://doi.org/10.1103/PhysRevLett.97.087204)

PACS numbers: 75.30.Et, 75.40.-s, 75.50.Ee, 78.30.-j

During the last decade the fascinating physics of spinel compounds came into the focus of modern solid-state physics and materials science. The classical and still unsolved nature of the Verwey transition in magnetite, where charge and orbital order compete [1], the heavy fermion behavior in LiV_2O_4 [2], the emergence of self-organized spin loops in ZnCr_2O_4 [3], colossal magnetoresistance in Cu doped FeCr_2S_4 [4] and gigantic Kerr rotation in FeCr_2S_4 [5], an orbital glass state in FeCr_2S_4 [6] and a spin-orbital liquid in FeSc_2S_4 [7], multiferroic behavior and colossal magnetocapacitive effect in CdCr_2S_4 and HgCr_2S_4 [8], spin dimerization in CuIr_2S_4 [9] and MgTi_2O_4 [10], and the spin-Peierls-like transitions in three-dimensional solids [11,12] are the most representative examples of exotic phenomena and ground states recently found in spinel compounds. The appearance of these fascinating ground states is attributed to the competition of charge, spin, and orbital degrees of freedom, which are strongly coupled to the lattice. In addition, both *A* and *B* sites in the normal AB_2X_4 spinels are geometrically frustrated. Within the *B* sublattice further complexity is emerging due to the competition of nearest neighbor (NN) ferromagnetic (FM) with direct, as well as next-nearest neighbor (NNN), antiferromagnetic (AFM) exchange. Hence, depending only on the *B*-site separation, FM and AFM ground states can be found [13,14], and in some cases FM and AFM exchange interactions are of equal strength leading to strong frustration.

In this Letter we present a detailed investigation of ZnCr_2S_4 , comparing our results with those of other Zn-Cr spinels. In these compounds Cr^{3+} reveals a half-filled t_{2g} ground state with almost zero spin-orbit coupling. Despite the fact that oxide, sulfide, and selenide are governed by different exchange interactions, as indicated by their Curie-Weiss (CW) temperatures, they reveal similar magnetic transition temperatures into AFM states: ZnCr_2O_4 , with the smallest Cr-Cr separation, has a negative CW temperature $\Theta = -390$ K and exhibits a transition from a paramagnet with strong quantum fluctuations

into a planar antiferromagnet at $T_N = 12.5$ K, accompanied by a small tetragonal distortion [3,11,15]. The oxide is governed by direct AFM Cr-Cr exchange [16]. The frustration parameter $f = \Theta/T_N \sim 30$ signals strong geometrical frustration [17]. The structural phase transition has been interpreted in terms of a spin Jahn-Teller effect [11,12,18]. The selenide, ZnCr_2Se_4 , with the largest Cr-Cr distance of the Zn-Cr spinels, has a positive $\Theta = 115$ K and exhibits a helical AFM structure below 20 K [13]. The helical structure is characterized by FM (001) planes with a propagation vector along the [001] axis [19]. The increase of the lattice constant in the selenide almost suppresses the direct exchange, and the spin arrangement follows from the dominating ferromagnetic 90° Cr-Se-Cr exchange and the additional AFM NNN Cr-Se-Zn-Se-Cr and Cr-Se-Se-Cr exchange. Again, the magnetic phase transition is accompanied by a small tetragonal distortion with $1 - c/a = 0.001$ [20].

The sulfide, ZnCr_2S_4 , lies exactly in between these two extremes. Consequently, FM and AFM exchange interactions almost compensate each other, yielding a CW temperature of approximately 0 K. Neutron diffraction [21] reveals a magnetic transition at 15.5 K into a helical spin order very similar to that in the selenide. Below 12 K a second commensurate collinear antiferromagnetic phase gradually developed down to 8 K. This second phase has a similar spin arrangement like the AFM oxide. At low temperatures both magnetic phases coexist [21], indicating that both spin structures are characterized by almost the same free energy. The metastable magnetic ground state comes along with the competing FM and AFM exchange of almost equal strength, a situation we term as bond frustration. So far structural phase transitions in ZnCr_2S_4 have not been reported to occur along with the magnetic transitions. In Ref. [21] an upper limit of $1 - c/a < 0.002$ has been established. However, we would like to note that in all Zn-Cr spinels the structural phase transition yields marginal distortions only and can hardly be detected using standard diffraction techniques. Here we use infrared spec-

troscopy to probe structural transitions and spin-lattice correlations.

Polycrystalline ZnCr_2S_4 was prepared by solid-state reaction from high purity elements at 800°C . X-ray diffraction analysis revealed single-phase material with the cubic spinel structure with a lattice constant $a = 9.983(2) \text{ \AA}$ and a sulfur fractional coordinate $x = 0.258(1)$. The susceptibility was measured using a commercial SQUID magnetometer. The heat capacity was monitored in a Quantum Design PPMS for temperatures $2 \text{ K} < T < 300 \text{ K}$ and in magnetic fields up to 70 kOe. The thermal expansion was measured by capacitive method in fields up to 70 kOe. The reflectivity experiments were carried out in the far infrared (FIR) range using the Fourier-transform spectrometer Bruker IFS 113v in a He bath cryostat.

Figure 1 presents the inverse susceptibility χ^{-1} vs temperature. For $T > 100 \text{ K}$, χ follows a CW law with a positive $\Theta \approx 8 \text{ K}$ and an effective moment of $3.86 \mu_B$, in good agreement with the spin-only value of Cr^{3+} in $3d^3$ configuration. In preliminary ESR experiments we determined a g value of 1.98, indeed indicating negligible spin-orbit coupling. Below 100 K, $\chi^{-1}(T)$ deviates from the FM CW law suggesting an increasing contribution of the AFM spin correlations. At 15 K, $\chi^{-1}(T)$ shows a clear minimum. This temperature marks the onset of long-range AFM order at T_{N1} [21].

The inset in Fig. 1 provides a closer look at the transition region. In a narrow temperature range around T_{N1} , our results are similar to those obtained in [21]. However, below T_{N1} , after a continuous drop, the susceptibility exhibits a sharp change of slope at around $T_{N2} = 8 \text{ K}$. In addition, we observed a pronounced difference between the susceptibilities measured on cooling and heating being maximal at T_{N2} . Such a hysteresis indicates a first-order

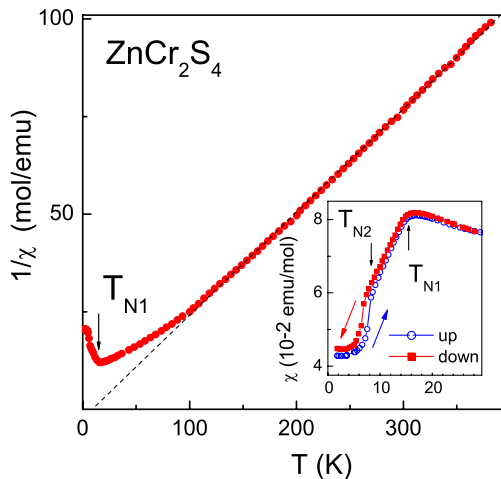


FIG. 1 (color online). Inverse susceptibility vs temperature as measured in ZnCr_2S_4 at 10 kOe. The dashed line indicates a CW behavior. Inset: Low-temperature susceptibility for heating (up) and cooling (down) cycles.

transformation. Both magnetic anomalies are in good agreement with the early neutron-diffraction experiments [21]. In the following we demonstrate that they correlate with respective anomalies found in the specific heat, thermal expansion, and IR spectra.

Figure 2(a) shows the specific heat in the representation C/T vs temperature at different magnetic fields. On approaching the Néel temperature T_{N1} , the specific heat manifests a sharp λ -type anomaly. At lower T , a second anomaly at T_{N2} becomes evident as a peak on heating and a kink on cooling. Note that this is the ordinary way in which the hysteresis at a first-order transition becomes visible in the relaxation method used [22]. The anomaly at T_{N2} in C/T correlates with the respective anomaly observed in the susceptibility. Strong spin-lattice coupling and possible structural instabilities connected with both magnetic transitions can be deduced from the thermal expansion which exhibits significant anomalies both at T_{N1} and T_{N2} [Fig. 2(b)]. In zero magnetic field the thermal-expansion coefficient α at T_{N2} is by a factor of 4 larger and again reveals a significant hysteresis in accordance with the first-order character and, thus, the importance of the spin-lattice correlations. Magnetic field has a strong effect on the specific heat and thermal expansion. It shifts the maximum in C/T at T_{N1} to lower temperatures as usually observed in antiferromagnets. A shift to lower T is found also for the maximum in α at T_{N1} which, in addition, shows an increase in the peak height. At the same time, at T_{N2} the peaks in C/T and α become strongly suppressed above fields of 20 kOe. Assuming that the peak in α at T_{N1} is related to the onset of a helical structure, its field dependence [Fig. 2(b)] suggests a stabilization of the helical spin

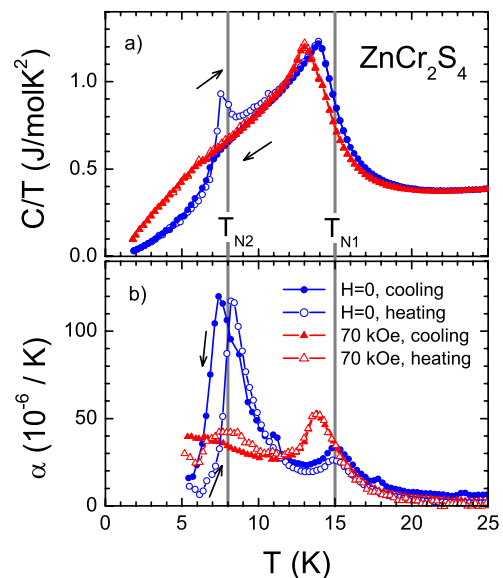


FIG. 2 (color online). (a) Heat capacity of ZnCr_2S_4 plotted as C/T vs T measured on cooling (closed symbols) and heating (open symbols) for 0 and 70 kOe. (b) Temperature dependence of the thermal-expansion coefficient at different magnetic fields. Vertical lines: the phase transitions T_{N1} and T_{N2} in zero field.

arrangement in the field. We note that the overall magnetic structure is AFM, however, the magnetic field favors the helical configuration due to the induced FM component. This corroborates our interpretation that the helical spin structure in ZnCr_2S_4 is supported by FM exchange, as already documented in ZnCr_2Se_4 , which has a large and positive CW temperature and reveals a helical spin structure as stable ground state. At the same time, the collinear structure below T_{N2} is supported by AFM exchange, in close analogy to strongly geometrically frustrated ZnCr_2O_4 . In ZnCr_2S_4 , the external magnetic fields break the balance of FM and AFM exchange interactions in favor of FM exchange and, hence, stabilizes the helical spin arrangement as revealed by the specific-heat and thermal-expansion experiments. The existence of strong spin-phonon coupling, which follows from the thermal-expansion data, is microscopically probed by means of IR spectroscopy.

For spinel compounds which show strong spin-phonon coupling effects [23–26] it is well established that the sign of shift of the phonon eigenfrequencies in the magnetically ordered state primarily depends on the type of coupling: FM or AFM, with the latter revealing positive shifts of the eigenfrequencies [25,26]. The main magnetic coupling mechanism in sulfides is superexchange which includes NN FM Cr-S-Cr and NNN AFM Cr-S-Zn-S-Cr or Cr-S-S-Cr exchange interactions [13,14]. From a thorough eigenmode analysis [24] it is known that the low-lying modes involve vibration of the Zn-S units, while Cr-S units are mostly involved in the high-frequency modes.

For the spinels with FM ground states like CdCr_2S_4 , as well as for ferrimagnetic FeCr_2S_4 , it has been demonstrated that the low-lying modes reveal large and positive shifts due to AFM exchange, while negative shifts have been observed for the high-frequency modes [25,26]. But in this case no splitting of the phonon modes could be detected at T_C , which seems to be clear as the FM spin order does not involve any lattice-symmetry breaking. A significant phonon splitting has been reported at the AFM phase transition in ZnCr_2O_4 , which is accompanied by a small tetragonal distortion [27]. Recently, this phonon splitting has been interpreted as driven only by spin correlations in the collinear AFM spin structure, where the magnetically induced symmetry breaking appears only in the dynamic phonon properties, but preserving the cubic structure [28]. The effect of phonon splitting due to magnetic ordering even in the absence of any structural symmetry breaking has been predicted earlier in [29].

Our room-temperature IR results on ZnCr_2S_4 are in good agreement with previously published data [30]. The IR spectrum reveals the four group-theoretically allowed phonon modes. A fit using a sum of Lorentz oscillators yields eigenfrequencies at 115, 244, 336, and 388 cm^{-1} . On decreasing temperature we find a positive frequency shift of the phonon eigenmodes, but below the magnetic transition temperatures all phonon modes reveal a clear splitting indicating a symmetry breaking as illustrated in

Fig. 3. The eigenfrequency for all phonon modes as a function of temperature is presented in Fig. 4 on a semi-logarithmic plot. From 300 K down to 20 K, the purely anharmonic behavior of a cubic spinel naturally describes the results. Below the first magnetic transition into the helical structure all main modes reveal an additional shift towards higher frequencies, as expected for AFM transitions. The shift is of the order of 0.5% for the high and of the order of 1% for the low-frequency modes. As the most important result we find that the splitting of the phonon modes does not occur at the same temperature: The high-frequency modes reveal splitting certainly at $T_{N1} = 15$ K: A weak but clearly pronounced shoulder is visible already at 14 K. At 5 K the splitting of both high-frequency phonons amounts to approximately 1%. On the contrary, the two low-frequency modes split distinctly below T_{N1} . The splitting results in extra peaks for both modes and in a pronounced shoulder for the phonon at 260 cm^{-1} , which indicates a splitting into three modes at low T . The overall splitting is of the order of 5% for both low-frequency modes.

The splitting of the IR-active modes in ZnCr_2S_4 at the two magnetic phase transitions further supports our interpretation. As outlined above, the high-frequency modes involve vibrations mostly of Cr-S units. The FM 90° Cr-S-Cr exchange governs the helical order of FM (001) planes. This exchange interaction is responsible for the splitting of the high-frequency modes. But ZnCr_2S_4 is equally dominated by AFM exchange which establishes the complex commensurate collinear spin order. These AFM interactions involve mainly Zn-S bonds which on the other side are involved in eigenfrequencies of the low-lying modes: Consequently, at T_{N2} these modes are expected to split as we experimentally observed. The comparable splitting of both high- and low-frequency modes ($\sim 5 \text{ cm}^{-1}$) provides compelling evidence that FM and AFM exchange interactions are of equal strength. The ground state energies of the two spin configurations are similar and the transition into the low-temperature phase is generated by these competing

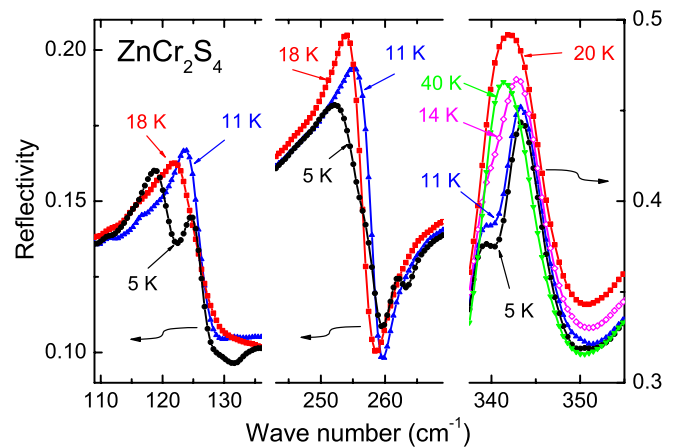


FIG. 3 (color online). Reflectivity for three phonon modes of ZnCr_2S_4 at temperatures around the magnetic transitions.

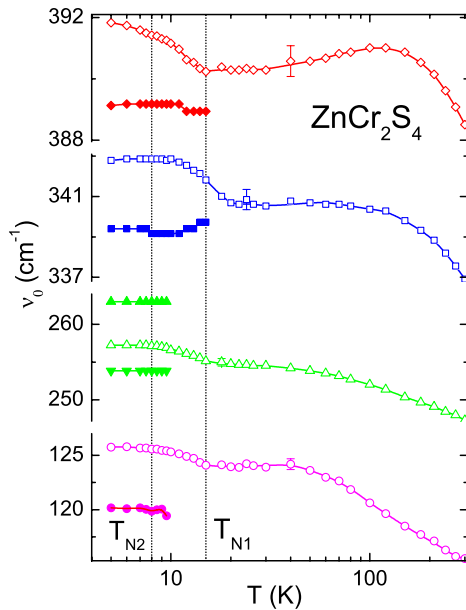


FIG. 4 (color online). Temperature dependence of the eigenfrequencies of the all phonon modes on a semilogarithmic plot. Open symbols: fundamental modes; closed symbols: the new modes below T_{N1} and T_{N2} .

interactions. Preliminary experiments in external magnetic fields show that the splitting of the low-frequency phonon modes is strongly suppressed for fields above 50 kOe. This observation is in agreement with the reduction of the anomalies of the specific heat and thermal expansion at T_{N2} by a magnetic field. Thus, our experiments prove that the low-temperature symmetry breaking in the Zn-Cr spinels mainly results from a strong spin-phonon coupling. This has been established for the geometrically frustrated ZnCr_2O_4 and we demonstrate this for the bond frustrated ZnCr_2S_4 . It will be highly interesting to see if the phonon splitting is accompanied by two consecutive structural transformations into low-symmetry structural phases, or if the symmetry breaking can only be observed via dynamic variables. High-resolution synchrotron experiments on single crystals will probably be necessary to solve this question.

In conclusion, we investigated the bond-frustrated AFM spinel ZnCr_2S_4 and found a splitting of high-frequency phonons below the onset of the antiferromagnetic helical order and splitting of the low-frequency modes at around the second magnetic transition into the collinear commensurate phase. Magnetic susceptibility, specific heat, and thermal expansion show an additional anomaly at the second transition beside the anomaly at the Néel point. Our results reveal strong spin-phonon coupling that generates the low-temperature structural instability in ZnCr_2S_4 . Suppression of the splitting of low-frequency phonons, and concomitantly of the anomalies, in the spe-

cific heat and thermal expansion by strong magnetic fields suggests a spin-driven origin of this transformation.

We are grateful to D. Vieweg, V. Fritsch, N. Tristan, and T. Wiedenmann for experimental support. This work was supported by BMBF via VDI/EKM, FKZ 13N6917-B and by DFG within SFB 484 (Augsburg).

*Corresponding author.

- [1] D.J. Huang *et al.*, Phys. Rev. Lett. **93**, 077204 (2004); I. Leonov *et al.*, Phys. Rev. Lett. **93**, 146404 (2004).
- [2] S. Kondo *et al.*, Phys. Rev. Lett. **78**, 3729 (1997); A. Krimmel *et al.*, Phys. Rev. Lett. **82**, 2919 (1999).
- [3] S.-H. Lee *et al.*, Nature (London) **418**, 856 (2002).
- [4] A.P. Ramirez, R.J. Cava, and J. Krajewski, Nature (London) **386**, 156 (1997); V. Fritsch *et al.*, Phys. Rev. B **67**, 144419 (2003).
- [5] K. Ohgushi *et al.*, Phys. Rev. B **72**, 155114 (2005).
- [6] R. Fichtl *et al.*, Phys. Rev. Lett. **94**, 027601 (2005).
- [7] V. Fritsch *et al.*, Phys. Rev. Lett. **92**, 116401 (2004); A. Krimmel *et al.*, Phys. Rev. Lett. **94**, 237402 (2005).
- [8] J. Hemberger *et al.*, Nature (London) **434**, 364 (2005); S. Weber *et al.*, Phys. Rev. Lett. **96**, 157202 (2006).
- [9] P.G. Radaelli *et al.*, Nature (London) **416**, 155 (2002).
- [10] M. Schmidt *et al.*, Phys. Rev. Lett. **92**, 056402 (2004).
- [11] S.-H. Lee *et al.*, Phys. Rev. Lett. **84**, 3718 (2000).
- [12] O. Tchernyshyov *et al.*, Phys. Rev. Lett. **88**, 067203 (2002).
- [13] N. Menyuk *et al.*, J. Appl. Phys. **37**, 1387 (1966).
- [14] K. Baltzer *et al.*, Phys. Rev. **151**, 367 (1966).
- [15] J.-H. Chung *et al.*, Phys. Rev. Lett. **95**, 247204 (2005).
- [16] J.B. Goodenough, Phys. Rev. **117**, B1442 (1960).
- [17] A.P. Ramirez, in *Handbook of Magnetic Materials*, edited by K.H.J. Buschow (Elsevier Science, Amsterdam, 2001), Vol. 13, p. 423.
- [18] Y. Yamashita and K. Ueda, Phys. Rev. Lett. **85**, 4960 (2000).
- [19] R. Plumier, J. Phys. (France) **27**, 213 (1966).
- [20] R. Kleinberger and R. de Kouchkovsky, C.R. Acad. Sci. Paris **262**, 628 (1966); M. Hidaka *et al.*, Phys. Status Solidi B **236**, 570 (2003).
- [21] M. Hamedoun *et al.*, J. Phys. C **19**, 1783 (1986); M. Hamedoun *et al.*, J. Phys. C **19**, 1801 (1986).
- [22] J. Hemberger *et al.*, Phys. Rev. B **72**, 012420 (2005); J.C. Lashley *et al.*, Cryogenics **43**, 369 (2003).
- [23] W. Baltensperger and J.S. Helman, Helv. Phys. Acta **41**, 668 (1968); W. Baltensperger, J. Appl. Phys. **41**, 1052 (1970).
- [24] P. Bruesch and F. D'Ambrogio, Phys. Status Solidi B **50**, 513 (1972).
- [25] K. Wakamura and T. Arai, J. Appl. Phys. **63**, 5824 (1988).
- [26] K. Wakamura Solid State Commun. **71**, 1033 (1989); T. Rudolf *et al.*, Phys. Rev. B **72**, 014450 (2005).
- [27] A.B. Sushkov *et al.*, Phys. Rev. Lett. **94**, 137202 (2005).
- [28] C.J. Fennie and K. Rabe, Phys. Rev. Lett. **96**, 205505 (2006).
- [29] S. Massidda *et al.*, Phys. Rev. Lett. **82**, 430 (1999).
- [30] H.D. Lutz *et al.*, J. Solid State Chem. **48**, 196 (1983).